Science in China Series F: Information Sciences

www.scichina.com
info.scichina.com
www.springerlink.com

Adaptive guidance law design based on characteristic model for reentry vehicles

YANG JunChun†, HU Jun & NI MaoLin

National Laboratory of Space Intelligent Control, Beijing Institute of Control Engineering, Beijing 100080, China

In this paper an adaptive guidance law based on the characteristic model is designed to track a reference drag acceleration for reentry vehicles like the Shuttle. The characteristic modeling method of linear constant systems is extended for single-input and single-output (SISO) linear time-varying systems so that the characteristic model can be established for reentry vehicles. A new nonlinear differential golden-section adaptive control law is presented. When the coefficients belong to a bounded closed convex set and their rate of change meets some constraints, the uniformly asymptotic stability of the nonlinear differential golden-section adaptive control system is proved. The tracking control law, the nonlinear differential golden-section control law, and the revised logical integral control law are integrated to design an adaptive guidance law based on the characteristic model. This guidance law overcomes the disadvantage of the feedback linearization method which needs the precise model. Simulation results show that the proposed method has better performance of tracking the reference drag acceleration than the feedback linearization one.

characteristic model, nonlinear differential golden-section control law, logical integral control law, adaptive guidance, asymptotic stability, reentry vehicles

1 Introduction

Guidance for reentry vehicles has attracted wide attention for a long time. For various vehicles, tasks, and requirements, the purpose of guidance is various. Therefore, the guidance method is largely different. Though the guidance laws in refs. [1, 2] have good performance for missiles and vehicles which attack fixed targets on the earth surface, they are not applicable to reentry vehicles like the Shuttle. These vehicles must satisfy many constraints to land safely for the high speed during reentry. All the constraints specify the reentry corridor. For simplicity, a piecewise linear

Received May 9, 2007; accepted December 26, 2007
doi: 10.1007/s11432-008-0109-y
†Corresponding author (email: yangjunchun@163.com)
Supported by the National Natural Science Foundation of China (Grant No. 90405017) and the "973" Program (Grant No. 2002CB312205)

reference drag acceleration vs. speed profile is designed within the corridor to satisfy all the constraints and range requirement. A linear feedback guidance method[3] for the Shuttle and a feedback linearization method[4−6] for nonlinear systems are used. In ref. [7], an auxiliary variable is defined and then the predictive control method is used. All the methods above have a common characteristic, which is to make the second-order error dynamic equations have good performances by canceling out the nonlinearity exactly and choosing an appropriate frequency and damping ratio. Due to the strong nonlinearity and coupling characteristic of systems, it is difficult to obtain the precise model and the nonlinearity cannot be cancelled exactly so that the controller performs badly. Adaptive control can adapt to parameter variations, but it is not applicable to the transition phase. To overcome this disadvantage, an all-coefficient adaptive control method is proposed from the viewpoint of engineering application[8]. Subsequently, a new modeling method —characteristic modeling is proposed to overcome the modeling difficulty in control system[9]. The characteristic modeling is to model by combining the dynamic characteristics of the controlled device with the control performance requirements. When the input is the same, the output of the characteristic model is equivalent to that of the real object. That is to say, the output error is within the permissible bounds during the transient phase and is zero after the steady state has been reached. The all-coefficient adaptive control based on the characteristic model provides a new idea for modeling and control of complex systems. This method has been applied to reentry control of manned spacecraft and obtained good performances[10].

In this paper, an adaptive guidance law based on the characteristic model is designed to track a reference drag acceleration profile for reentry vehicles like the Shuttle. Firstly, the characteristic modeling method for linear constant systems is extended for SISO linear time-varying systems so that the characteristic model can be established for reentry vehicles. Then, a new nonlinear differential golden-section adaptive control law is proposed. When the coefficients belong to a bounded closed convex set and their rate of change meets some constraints, the uniformly asymptotic stable sufficient condition of the nonlinear differential golden-section adaptive control system is given. That is to say, the coefficient variations of the closed loop system must satisfy constraints (44)—(46). The tracking control law, the nonlinear differential golden section control law and the revised logical integral control law are integrated to design an adaptive guidance law based on the characteristic model. This guidance law overcomes the disadvantage of the feedback linearization method that needs the precise model. Simulation results show that the proposed method has better performance of tracking the reference drag acceleration than the feedback linearization one has.

2 Drag acceleration derivation

The motion equations for reentry vehicles in the vertical plane are[11]

$$\dot{h} = v\sin\theta, \tag{1}$$

$$\dot{v} = -\rho(r)SC_D(\alpha, Ma)v^2/(2m) - g(r)\sin\theta, \tag{2}$$

$$\dot{\theta} = \rho(r)SC_L(\alpha, Ma)v\cos\sigma/(2m) - g(r)\cos\theta/v + v\cos\theta/r, \tag{3}$$

where h is the height, v is the velocity, θ is the flight path angle, r is the radius from the center of the earth to the vehicle, S is the reference area, m is the mass, α is the angle of

attack, σ is the bank angle, Ma is the Mach number. $C_L(\alpha, Ma)$ is the lift coefficient, $C_D(\alpha, Ma)$ is the drag coefficient. Both of them are the functions of α and Ma. $\rho(r)$ is the atmosphere density, $g(r)$ is the gravity acceleration of the earth. Both of them are the functions r. For written simplicity, $C_L(\alpha, Ma)$, $C_D(\alpha, Ma)$, $g(r)$ and $\rho(r)$ are replaced respectively by C_L, C_D, g and ρ in the following. a_D is the drag acceleration; L is the lift; D is the drag; $L/D = C_L/C_D$ is the lift-drag ratio. Input u is the vertical component of the lift-drag ratio. The expressions for the above variables are

$$u = (L/D)_V = (L/D)\cos\sigma = (C_L/C_D)\cos\sigma, \tag{4}$$

$$h = r - R_0, \tag{5}$$

$$\rho = \rho_0 e^{-h/h_s}, \tag{6}$$

$$a_D = \rho S C_D v^2/(2m), \tag{7}$$

$$g = R_0^2 g_0 / r^2, \tag{8}$$

where R_0 is the mean radius of the earth, g_0 is the gravity acceleration at the standard sea level, h_s is a constant. The purpose of guidance is to control vehicles to track a designed reference drag acceleration profile. Therefore, the drag acceleration a_D is chosen as the system output. Using eqs. (4) and (7), the derivatives of v and θ follow from eqs. (2) and (3) as

$$\dot{v} = -a_D - g\sin\theta, \tag{9}$$

$$\dot{\theta} = a_D u/v - g\cos\theta/v + v\cos\theta/r. \tag{10}$$

Then, the derived input-output dynamics is represented as

$$\begin{aligned}\ddot{a}_D = {} & \frac{\dot{a}_D^2}{a_D} - 2\frac{a_D\dot{a}_D}{v} - \frac{2a_D^3}{v^2} + \frac{2a_D g^2}{v^2} - \frac{2a_D g}{r} - \frac{a_D v^2}{h_s r} + \frac{a_D g}{h_s} + \frac{a_D\ddot{C}_D}{C_D} - \frac{a_D\dot{C}_D^2}{C_D^2} \\ & + \sin^2\theta\left(-\frac{4a_D g^2}{v^2} + \frac{6a_D g}{r} + \frac{a_D v^2}{h_s r}\right) + \sin\theta\left(\frac{a_D^2}{h_s} - \frac{4a_D^2 g}{v^2}\right) + u\left(-\frac{2ga_D^2}{v^2} - \frac{a_D^2}{h_s}\right)\cos\theta. \end{aligned} \tag{11}$$

The detailed derivation of eq. (11) is in Appendix of this paper. Due to the small θ during reentry flight, letting[3] $\sin\theta \approx 0, \cos\theta \approx 1$, eq. (11) becomes eq. (12),

$$\ddot{a}_D = \frac{\dot{a}_D^2}{a_D} - 2\frac{a_D\dot{a}_D}{v} - \frac{2a_D^3}{v^2} + \frac{2a_D g^2}{v^2} - \frac{2a_D g}{r} - \frac{a_D v^2}{h_s r} + \frac{a_D g}{h_s} + \frac{a_D\ddot{C}_D}{C_D} - \frac{a_D\dot{C}_D^2}{C_D^2} + \left(-\frac{2ga_D^2}{v^2} - \frac{a_D^2}{h_s}\right)u. \tag{12}$$

3 Perturbation equation of the drag acceleration

In eq. (12), the input-output relationship is a nonlinear function. Small deviations from the reference values are defined as

$$\Delta\ddot{a}_D \triangleq \ddot{a}_D - \ddot{a}_{D_0},\ \Delta\dot{a}_D \triangleq \dot{a}_D - \dot{a}_{D_0},\ \Delta a_D \triangleq a_D - a_{D_0},\ \Delta v \triangleq v - v_0,\ \Delta u \triangleq u - u_0.$$

Differentiating eq. (12),

$$\delta\ddot{a}_D=\left(\frac{2\dot{a}_{D_0}}{a_{D_0}}-\frac{2a_{D_0}}{v_0}\right)\delta\dot{a}_D+\left[-\frac{\dot{a}_{D_0}^2}{a_{D_0}^2}-\frac{2\dot{a}_{D_0}}{v_0}-\frac{6a_{D_0}^2}{v_0^2}+\frac{2g^2}{v_0^2}-\frac{2g}{r_0}-\frac{v_0^2}{h_sr_0}+\frac{g}{h_s}+\frac{\ddot{C}_{D_0}}{C_{D_0}}-\frac{\dot{C}_{D_0}^2}{C_{D_0}^2}\right.$$
$$\left.-\frac{4ga_{D_0}}{v_0^2}u_0-\frac{2a_{D_0}}{h_s}u_0\right]\delta a_D+\left[\frac{4a_{D_0}^3}{v_0^3}-\frac{4a_{D_0}g^2}{v_0^3}-\frac{2a_{D_0}v_0}{h_sr_0}+\frac{2a_{D_0}\dot{a}_{D_0}}{v_0^2}+\frac{4ga_{D_0}^2}{v_0^3}u_0\right]\delta v+\frac{a_{D_0}}{C_{D_0}}\delta\ddot{C}_D$$
$$-\frac{2a_{D_0}\dot{C}_{D_0}}{C_{D_0}^2}\delta\dot{C}_D+\left(\frac{2a_{D_0}\dot{C}_{D_0}^2}{C_{D_0}^3}-\frac{a_{D_0}\ddot{C}_{D_0}}{C_{D_0}^2}\right)\delta C_D+\left(-\frac{2g}{v_0^2}-\frac{1}{h_s}\right)a_{D_0}^2\delta u, \tag{13}$$

where the subscript 0 represents the reference values. With Earth-relative speed chosen as the independent variable, $\delta v=0$. During reentry flight, bank angle modulation is used for ranging. Therefore, (see ref. [3]) $\delta\ddot{C}_D=0,\quad \delta\dot{C}_D=0,\quad \delta C_D=0.$ Then, eq. (13) becomes

$$\delta\ddot{a}_D=\left(\frac{2\dot{a}_{D_0}}{a_{D_0}}-\frac{2a_{D_0}}{v_0}\right)\delta\dot{a}_D+\left[-\frac{\dot{a}_{D_0}^2}{a_{D_0}^2}-\frac{2\dot{a}_{D_0}}{v_0}-\frac{6a_{D_0}^2}{v_0^2}+\frac{2g^2}{v_0^2}-\frac{2g}{r_0}-\frac{v_0^2}{h_sr_0}+\frac{g}{h_s}\right.$$
$$\left.+\frac{\ddot{C}_{D_0}}{C_{D_0}}-\frac{\dot{C}_{D_0}^2}{C_{D_0}^2}-\frac{4ga_{D_0}}{v_0^2}u_0-\frac{2a_{D_0}}{h_s}u_0\right]\delta a_D+\left(-\frac{2g}{v_0^2}-\frac{1}{h_s}\right)a_{D_0}^2\delta u. \tag{14}$$

Since a_{D_0},v_0,r_0 are time-varying, eq. (14) can be represented equivalently as

$$\delta\ddot{a}_D=a_1(t)\delta\dot{a}_D+a_0(t)\delta a_D+b(t)\delta u, \tag{15}$$

where

$$a_1(t)=2\dot{a}_{D_0}/a_{D_0}-2a_{D_0}/v_0, \tag{16}$$

$$a_0(t)=-\frac{\dot{a}_{D_0}^2}{a_{D_0}^2}-\frac{2\dot{a}_{D_0}}{v_0}-\frac{6a_{D_0}^2}{v_0^2}+\frac{2g^2}{v_0^2}-\frac{2g}{r_0}-\frac{v_0^2}{h_sr_0}+\frac{g}{h_s}+\frac{\ddot{C}_{D_0}}{C_{D_0}}-\frac{\dot{C}_{D_0}^2}{C_{D_0}^2}-\frac{4ga_{D_0}}{v_0^2}u_0-\frac{2a_{D_0}}{h_s}u_0, \tag{17}$$

$$b(t)=\left(-2g/v_0^2-1/h_s\right)a_{D_0}^2. \tag{18}$$

4 Characteristic model establishment

To obtain the characteristic model of eq. (15), the SISO linear time-varying system in the form of eq. (19) is modeled first. The derivation is similar to that of ref. [12].

$$x^{(n)}=a_0(t)x+a_1(t)\dot{x}+\cdots+a_{n-1}(t)x^{(n-1)}+b(t)u(t). \tag{19}$$

Assume that $a_i(t),\quad b(t),\quad x(t)$, and the derivatives of $x(t)$ are all bounded in eq. (19). The following is derived from eq. (19).

$$\begin{aligned}\dot{x}&=a_0(t)x+a_1(t)\dot{x}+\cdots+a_{n-1}(t)x^{(n-1)}-x^{(n)}+\dot{x}+b(t)u(t)\\&=a_0(t)x+b(t)u(t)+F\left(\dot{x},\cdots,x^{(n)}\right),\end{aligned} \tag{20}$$

where

$$F\left(\dot{x},\cdots,x^{(n)}\right)=a_1(t)\dot{x}+\cdots+a_{n-1}(t)x^{(n-1)}-x^{(n)}+\dot{x}.$$

Differentiating eq. (20),

$$\ddot{x} = \dot{a}_0(t)x + a_0(t)\dot{x} + \dot{b}(t)u(t) + b(t)\dot{u}(t) + \mathrm{d}F\left(\dot{x}, \cdots, x^{(n)}\right)/\mathrm{d}t. \tag{21}$$

Making difference of eq. (20),

$$\frac{x(k)-x(k-1)}{\Delta t} = a_0(k)x(k) + b(k)u(k) + F(k). \tag{22}$$

Making difference of eq. (21)

$$\frac{x(k+1)-2x(k)+x(k-1)}{\Delta t^2} = \frac{a_0(k)-a_0(k-1)}{\Delta t}x(k) + a_0(k)\frac{x(k)-x(k-1)}{\Delta t}$$
$$+\frac{b(k)-b(k-1)}{\Delta t}u(k) + b(k)\frac{u(k)-u(k-1)}{\Delta t} + \frac{F(k)-F(k-1)}{\Delta t}. \tag{23}$$

Adding eqs. (22) to (23), then eq. (24) is derived.

$$x(k+1) = \left[2 + \left(a_0(k) - a_0(k-1)\right)\Delta t + a_0(k)\Delta t - \Delta t + a_0(k)\Delta t^2\right]x(k)$$
$$+\left[-1 - a_0(k)\Delta t + \Delta t\right]x(k-1) + \left[\left(b(k)-b(k-1)\right)\Delta t + b(k)\Delta t + b(k)\Delta t^2\right]u(k)$$
$$+\left[-b(k)\Delta t\right]u(k-1) + F(k)\Delta t^2 + \left[F(k)-F(k-1)\right]\Delta t. \tag{24}$$

Let

$$f_1(k) = 2 + \left(a_0(k) - a_0(k-1)\right)\Delta t + a_0(k)\Delta t - \Delta t + a_0(k)\Delta t^2,$$
$$f_2(k) = -1 - a_0(k)\Delta t + \Delta t,$$
$$g_0(k) = \left(b(k) - b(k-1)\right)\Delta t + b(k)\Delta t + b(k)\Delta t^2,$$
$$g_1(k) = -b(k)\Delta t,$$
$$W(k) = F(k)\Delta t^2 + [F(k) - F(k-1)]\Delta t.$$

If the constant control is desired, then $W(k) = 0$ at steady state, since $F(k)$ is the combination of the derivatives of x so that $F(k) = F(k-1) = 0$. During the transient phase, since the coefficients and derivatives of x in eq. (19) are all bounded, $F(k)$ and $F(k-1)$ are bounded. Assuming $|F(k)| < K$ (K is a constant), then $|W(k)| \leqslant 2K\Delta t + K\Delta t^2$. If $\Delta t \to 0$, then $W(k) \to 0$. Therefore, $W(k)$ can be treated as the modeling error during the transient phase. Then, the characteristic model of eq. (19) is

$$x(k+1) = f_1(k)x(k) + f_2(k)x(k-1) + g_0(k)u(k) + g_1(k)u(k-1). \tag{25}$$

Judging from the expression for $W(k)$, the smaller the sampled period is, the smaller the modeling error is during the transient phase. Given ε satisfying $\varepsilon > 0$, chosen Δt satisfying $0 < \Delta t < \delta$, where $\delta = \min\{1, \varepsilon/(3K)\}$, then

$$|W(k)| \leqslant 2K\Delta t + K\Delta t^2 = (2K + K\Delta t)\Delta t < (2K + K)\varepsilon/(3K) = \varepsilon.$$

From the above derivation, when the sampled period satisfies $0 < \Delta t < \delta$, the modeling error of the characteristic model is smaller than ε. In this sense, the characteristic model is equivalent to the original system. That is to say, when the inputs are the same, the outputs are equal during the steady phase and the errors are kept within permissible bounds during the transient phase. Therefore, the characteristic model reflects the characteristic of the original system.

Using the method above, the characteristic model of eq. (15) is established as follows. eq. (15) is written as

$$\ddot{x}(t) = a_1(t)\dot{x}(t) + a_0(t)x(t) + b(t)u(t), \tag{26}$$

where $x(t) = \delta a_D(t)$ and $a_1(t)$, $a_0(t)$, $b(t)$ are given by eqs. (16)—(18). Making difference of eq. (26),

$$\frac{x(k+1) - 2x(k) + x(k-1)}{\Delta t^2} = a_1(k)\frac{x(k) - x(k-1)}{\Delta t} + a_0(k)x(k) + b(k)u(k). \tag{27}$$

eq. (28) is derived from eq. (27).

$$x(k+1) = \alpha_1(k)x(k) + \alpha_2(k)x(k-1) + \beta(k)u(k), \tag{28}$$

where

$$\alpha_1(k) = 2 + a_1(k)\Delta t + a_0(k)\Delta t^2,$$
$$\alpha_2(k) = -1 - a_1(k)\Delta t,$$
$$\beta(k) = b(k)\Delta t^2.$$

Due to the simplification for derivation of eq. (14) and other effects (such as the aerodynamic coefficients and their derivatives cannot be obtained precisely; the atmosphere density is modeled approximately) the coefficients $\alpha_1(k)$, $\alpha_2(k)$ and $\beta(k)$ by the above expressions are not precise. The uncertainties can be compensated by estimating coefficients of the characteristic model (28) on line. Therefore, it is not necessary for characteristic modeling to know the precise dynamic model of the object.

The coefficients of the characteristic model (28) have the following characteristics:

1) $\alpha_i(k), i = 1, 2$, and $\beta(k)$ are time-varying.

Defining $\Delta_1 = \left|\frac{\alpha_i(k+1) - \alpha_i(k)}{\alpha_i(k)}\right|$ and $\Delta_2 = \left|\frac{\beta(k+1) - \beta(k)}{\beta(k)}\right|$, if $\Delta t \to 0$, then $\Delta_1 \to 0$, $\Delta_2 \to 0$.

2) If $\Delta t \to 0$, then $\alpha_1(k) \to 2$, $\alpha_2(k) \to -1$, and the sum of the coefficients in eq. (28) is equal to 1.

From expressions (16)—(18), we know $a_1(k)$, $a_0(k)$, $b(k)$ are bounded, then

$$\lim_{\Delta t \to 0} \alpha_1(k) = \lim_{\Delta t \to 0}[2 + a_1(k)\Delta t + a_0(k)\Delta t^2] = 2,$$
$$\lim_{\Delta t \to 0} \alpha_2(k) = \lim_{\Delta t \to 0}[-1 - a_1(k)\Delta t] = -1,$$
$$\lim_{\Delta t \to 0}[\alpha_1(k) + \alpha_2(k) + \beta(k)] = \lim_{\Delta t \to 0}[1 + a_0(k)\Delta t^2 + b(k)\Delta t^2] = 1.$$

Now, we have obtained the characteristic model (28) for the reentry vehicle whose input is the vertical component of the lift-drag ratio and output is drag acceleration.

In order to verify the input-output equivalent relationship between characteristic model (28) and the system (14), $u(t) = 1$ and $u = \sin(0.1\pi t)$ are chosen as the input signals in the simulation. The output of characteristic model (28) is $y_c(k) = x(k)$ and the output of system (14) is $y_m(t) = \delta a_D(t)$. The sampled period is $\Delta t = 0.1$ s. The simulation lasts for the whole reentry

period of the nominal trajectory. The output error between the characteristic model (28) and the system (14) at the sampled time is $e(k)=y_c(k)-y_m(k)$. When $u(t)=1$, the maximum output error is $e_{\max}=9.6\times10^{-5}$. When $u=\sin(0.1\,\pi t)$, the maximum error is $e_{\max}=1.1\times10^{-5}$. Therefore, the input-output relationship of the characteristic model and the original system is uniform within the given error bounds.

5 Nonlinear differential golden-section adaptive control and the stability analysis

When the slope of the tracked reference drag acceleration profile is changed abruptly, the overshoot cannot be avoided due to the high speed of the vehicle during reentry. If the differential coefficient is increased, the system damping ratio will be increased so that the tracking can converge quickly. Considering the tracking characteristic of the piecewise linear drag acceleration vs. velocity profile, a nonlinear differential golden-section adaptive control law is proposed as follows:

$$u_L(k)=-\left[\left(L_1\hat{\alpha}_1(k)+L_2\hat{\alpha}_2(k)\right)x(k)-L_2\hat{\alpha}_2(k)\left(\eta_1\left|x(k)\right|^{\mu}+\eta_2\right)\left(x(k)-x(k-1)\right)\right]\Big/\hat{\beta}(k), \quad (29)$$

where $L_1=0.382$, $L_2=0.618$ are golden-section coefficients; η_1,η_2 are positive constants and μ is a constant. The three constants can be chosen according to object features and control performance requirements. $\hat{\alpha}_1(k)$, $\hat{\alpha}_2(k)$, and $\hat{\beta}(k)$ are the estimated values of the corresponding coefficients in eq. (28). The coefficients are estimated by the gradient projection algorithm,

$$\hat{\theta}^*(k)=\hat{\theta}(k-1)+\frac{\lambda_1\phi(k-1)}{\lambda_2+\phi^{\mathrm{T}}(k-1)\phi(k-1)}\left[x(k)-\phi^{\mathrm{T}}(k-1)\hat{\theta}(k-1)\right], \quad (30)$$

$$\hat{\theta}(k)=\pi\left[\hat{\theta}^*(k)\right], \quad (31)$$

where $\hat{\theta}(k-1)=[\hat{\alpha}_1(k-1)\quad\hat{\alpha}_2(k-1)\quad\hat{\beta}(k-1)]^{\mathrm{T}}$; $\phi(k-1)=[x(k-1)\quad x(k-2)\quad u(k-1)]^{\mathrm{T}}$; λ_1, λ_2 are positive constants satisfying $0<\lambda_1<1$, $\lambda_2>0$; $\pi(x)$ represents the orthogonal projection from x to the bounded closed convex set D. D is related to discretization method and sampled period.

Defining

$$k_p=\left[L_1\hat{\alpha}_1(k)+L_2\hat{\alpha}_2(k)\right]/\hat{\beta}(k),$$

$$k_d=-L_2\hat{\alpha}_2(k)/\hat{\beta}(k),$$

$$K_D(k,x(k))=k_d\left[\eta_1\left|x(k)\right|^{\mu}+\eta_2\right],$$

then nonlinear differential golden-section adaptive control law (29) can be represented as

$$u_L(k)=-\left[k_p x(k)+K_D(k,x(k))\left(x(k)-x(k-1)\right)\right]. \quad (32)$$

The differential coefficient $K_D(k,x(k))$ is related to k_d and it varies with $\left|x(k)\right|$. Noticeably, the control law (29) proposed in this paper is different from that in ref. [13] which cannot satisfy

the requirement for high speed reentry vehicles of tracking the drag acceleration profile with abrupt change of slope.

The closed loop system which consists of the characteristic model (28), the parameter estimation algorithm (30)—(31) and the nonlinear differential golden-section adaptive control law (29) can be written as

$$x(k+1)+f_1(k,x(k))x(k)+f_2(k,x(k))x(k-1)=0, \tag{33}$$

where

$$f_1(k,x(k))=-\alpha_1(k)+\left[L_1\hat{\alpha}_1(k)+L_2\hat{\alpha}_2(k)-L_2\hat{\alpha}_2(k)\left(\eta_1|x(k)|^{\mu}+\eta_2\right)\right]\beta(k)/\hat{\beta}(k), \tag{34}$$

$$f_2(k,x(k))=-\alpha_2(k)+\left[L_2\hat{\alpha}_2(k)\left(\eta_1|x(k)|^{\mu}+\eta_2\right)\right]\beta(k)/\hat{\beta}(k). \tag{35}$$

Eq. (33) can be described as

$$X(k+1)=A(k+1,X(k+1))X(k), \tag{36}$$

where

$$A(k+1,X(k+1))=\begin{bmatrix}0 & 1\\ -f_2(k+1,x(k+1)) & -f_1(k+1,x(k+1))\end{bmatrix},$$

$$X(k)=\begin{bmatrix}x(k) & x(k+1)\end{bmatrix}^{\mathrm{T}}.$$

For written convenience, $f_1(k,x(k))$, $f_2(k,x(k))$, and $A(k,X(k))$ will be replaced respectively by $f_1(k)$, $f_2(k)$, and $A(k)$ in the subsequent part.

In order to analyze the stability of the closed loop system, several lemmas are given first.

Lemma 1[13]**.** The nonlinear time-varying system (33), whose origin is the equilibrium point, is uniformly asymptotic stable if given a uniformly bounded and positive definite matrix $P(k,X(k))$, that is to say, the constants $m_1>0$ and $M_1>0$ exist and $P(k,X(k))$ satisfies

$$m_1 I\leqslant P(k,X(k))\leqslant M_1 I. \tag{37}$$

$Q(k,X(k))$ determined by

$$A^{\mathrm{T}}(k+1,X(k+1))P(k+1,X(k+1))A(k+1,X(k+1))-P(k,X(k))=-Q(k,X(k)) \tag{38}$$

is uniformly bounded and positive definite, that is to say, the constants $m_2>0$ and $M_2>0$ exist and $Q(k,X(k))$ satisfies

$$m_2 I\leqslant Q(k,X(k))\leqslant M_2 I, \tag{39}$$

where I is a unit matrix with proper dimensions.

Lemma 2. Assuming that $B(k)=(b_{ij}(k))$ is an nth order real symmetrical matrix, if all the sequential leading minors of $B(k)$ are bounded and larger than some positive constant, then $B(k)$ is uniformly bounded and positive definite, that is to say, the constants $m>0$ and $M>0$ exist which make $B(k)$ satisfy $mI\leqslant B(k)\leqslant MI$.

Lemma 3[14]**.** Assuming $M_2(k)\in R$, $0<M_2(k)\leqslant M$, where M is a positive constant,

the quadratic trinomial of $Z(k)$ is

$$N(k) = -M_2(k)Z^2(k) + M_1(k)Z(k) + M_0(k), \tag{40}$$

whose discriminant is

$$\Delta(k) = M_1^2(k) + 4M_2(k)M_0(k). \tag{41}$$

Then,

(a) if $\Delta(k) > 0$ and $Z(k)$ satisfies

$$\frac{M_1(k) - \sqrt{\Delta(k)}}{2M_2(k)} < Z(k) < \frac{M_1(k) + \sqrt{\Delta(k)}}{2M_2(k)}, \tag{42}$$

then $N(k) > 0$.

(b) if $\Delta(k) > \varepsilon > 0$ and $Z(k)$ satisfies

$$\frac{M_1(k) - \sqrt{\Delta(k) - \varepsilon}}{2M_2(k)} < Z(k) < \frac{M_1(k) + \sqrt{\Delta(k) - \varepsilon}}{2M_2(k)}, \tag{43}$$

then $N(k) > \varepsilon/(4M)$.

The following stability theorem is for the system (33).

Theorem 1. Assuming $0 < \beta(k)/\hat{\beta}(k) \leqslant 2$ and $|x(k)|^{\mu} < M$, the closed loop system (33), which consists of the time-varying linear controlled device with unknown parameters which belong to a known bounded closed convex set D, the estimation algorithm (30)—(31) and the nonlinear differential golden-section adaptive control law (29), whose origin is the equilibrium point, is uniformly asymptotic stable, if

The change rate of $f_1(k)$ satisfies

$$\frac{N_1(k)}{2} - \sqrt{q_{11}(k)q_{22}(k) - \overline{\delta}} < -\varepsilon_1 \Delta f_1(k) < \frac{N_1(k)}{2} + \sqrt{q_{11}(k)q_{22}(k) - \overline{\delta}}, \tag{44}$$

The change rate of $f_1^2(k)$ and $f_2^2(k)$ satisfies

$$\Delta(f_1^2(k)) < -f_2^2(k+1) + (1 + 2\varepsilon_1 - \delta_2)f_1^2(k+1) - f_1^4(k+1) + \delta_2 - \delta_1 - \delta_{22}, \tag{45}$$

$$\Delta(f_2^2(k)) < (1 - \delta_2)f_2^2(k+1) - f_1^2(k+1)f_2^2(k+1) + \delta_1 - \delta_{11}, \tag{46}$$

where $0 < \delta_1 < \delta_2$, $0 < \delta_{11}$, $0 < \delta_{22}$, $0 < \overline{\delta} < \delta_{11}\delta_{22}$, $0 < \varepsilon_1 < \delta_1/(\sqrt{3}M_1)$, M_1 is the upper bound of $|f_1(k)|$, $\Delta f_1(k) = f_1(k+1) - f_1(k)$, $\Delta f_2(k) = f_2(k+1) - f_2(k)$, $\Delta(f_1^2(k)) = f_1^2(k+1) - f_1^2(k)$, $\Delta(f_2^2(k)) = f_2^2(k+1) - f_2^2(k)$.

$$N_1(k) = -2p_{12}(k+1) - 2[p_{12}(k+1)f_2(k+1) - p_{22}(k+1)f_1(k+1)f_2(k+1)], \tag{47}$$

$$\begin{cases} p_{11}(k) = f_2^2(k) + \delta_1, \\ p_{12}(k) = \varepsilon_1 f_1(k), \\ p_{22}(k) = f_1^2(k) + \delta_2, \end{cases} \tag{48}$$

$$\begin{cases} q_{11}(k) = p_{11}(k) - p_{22}(k+1) f_2^2(k+1), \\ q_{12}(k) = p_{12}(k) + p_{12}(k+1) f_2(k+1) - p_{22}(k+1) f_1(k+1) f_2(k+1), \\ q_{22}(k) = p_{22}(k) - p_{11}(k+1) + 2 p_{12}(k+1) f_1(k+1) - p_{22}(k+1) f_1^2(k+1), \end{cases} \tag{49}$$

Proof. For system (33), choose a Liapunov function as

$$V(k) = X^{\mathrm{T}}(k) P(k) X(k).$$

Combining eq. (36), then

$$\Delta V(k) = -X^{\mathrm{T}}(k) \left[P(k) - A^{\mathrm{T}}(k+1) P(k+1) A(k+1) \right] X(k). \tag{50}$$

According to Lemma 1, $Q(k)$ can be expressed as

$$Q(k) = P(k) - A^{\mathrm{T}}(k+1) P(k+1) A(k+1), \tag{51}$$

where

$$P(k) = \begin{bmatrix} p_{11}(k) & p_{12}(k) \\ p_{12}(k) & p_{22}(k) \end{bmatrix}, \tag{52}$$

$p_{11}(k)$, $p_{22}(k)$, $p_{12}(k)$ are given by eqs. (48).

$Q(k)$ follows from eq. (51) as

$$Q(k) = \begin{bmatrix} q_{11}(k) & q_{12}(k) \\ q_{12}(k) & q_{22}(k) \end{bmatrix}, \tag{53}$$

where $q_{11}(k)$, $q_{22}(k)$, and $q_{12}(k)$ are given by expression (49). Since $\alpha_1(k)$, $\alpha_2(k)$, and $\beta(k)$ belong to a known bounded closed convex set D, and estimation algorithms (30), (31) make $\hat{\alpha}_1(k)$, $\hat{\alpha}_2(k)$, and $\hat{\beta}(k)$ belong to the same D, according to the assumption $0 < \beta(k) / \hat{\beta}(k) \leqslant 2$ [15] and $|x(k)|^{\mu} < M$, using expressions (34), (35), $f_1(k)$ and $f_2(k)$ are bounded. That is to say, $M_1 > 0$ and $M_2 > 0$ which make

$$|f_1(k)| < M_1, \quad |f_2(k)| < M_2. \tag{54}$$

Since $f_1(k)$ and $f_2(k)$ are bounded, from expression (48), we can conclude that every element of $P(k)$ is bounded. And then, from eq. (49), every element of $Q(k)$ is bounded.

Step 1. Prove that $P(k)$ is uniformly bounded and positive definite.

The first order sequential leading minor of $P(k)$ is

$$M_{P_1} = p_{11}(k) = f_2^2(k) + \delta_1 > \delta_1. \tag{55}$$

The second order sequential leading minor of $P(k)$ is

$$M_{P_2} = p_{11}(k) p_{22}(k) - p_{12}^2(k) = \left(f_2^2(k) + \delta_1 \right) \left(f_1^2(k) + \delta_2 \right) - \varepsilon_1^2 f_1^2(k) > \delta_1^2 - \delta_1^2 / 3. \tag{56}$$

According to expressions (55), (56), M_{P_1} and M_{P_2} are larger than a positive constant. Since every element of $P(k)$ is bounded, then M_{P_1} and M_{P_2} are bounded. From Lemma 2, we can conclude that $P(k)$ is uniformly bounded and positive definite.

Step 2. Prove $Q(k)$ is uniformly bounded and positive definite.

Since

$$q_{11}(k) = -\Delta\left(f_2^2(k)\right) + (1-\delta_2) f_2^2(k+1) - f_1^2(k+1) f_2^2(k+1) + \delta_1, \tag{57}$$

using inequality (46), then $q_{11}(k) > \delta_{11}$.

Since

$$q_{22}(k) = -\Delta\left(f_1^2(k)\right) - f_2^2(k+1) + (1+2\varepsilon_1-\delta_2) f_1^2(k+1) - f_1^4(k+1) + \delta_2 - \delta_1, \tag{58}$$

using inequality (45) , then $q_{22}(k) > \delta_{22}$.

The first order sequential leading minor of $Q(k)$ is

$$M_{Q_1} = q_{11}(k) > \delta_{11}. \tag{59}$$

The second order sequential leading minor of $Q(k)$ is

$$M_{Q_2} = -\left[p_{12}(k) - p_{12}(k+1)\right]^2 + N_1(k)\left[p_{12}(k) - p_{12}(k+1)\right] + N_0(k), \tag{60}$$

where

$$N_1(k) = -2p_{12}(k+1) - 2\left[p_{12}(k+1) f_2(k+1) - p_{22}(k+1) f_1(k+1) f_2(k+1)\right], \tag{61}$$

$$\begin{aligned} N_0(k) &= p_{12}^2(k+1) + N_1(k) p_{12}(k+1) \\ &\quad -\left[p_{12}(k+1) f_2(k+1) - p_{22}(k+1) f_1(k+1) f_2(k+1)\right]^2 + q_{11}(k) q_{22}(k). \end{aligned} \tag{62}$$

Defining

$$\begin{aligned} &M(k) = 1, \quad B(k+1) = p_{12}(k+1), \quad F(k) = 0, \quad D(k) = q_{11}(k) q_{22}(k), \\ &C(k+1) = p_{12}(k+1) f_2(k+1) - p_{22}(k+1) f_1(k+1) f_2(k+1). \end{aligned}$$

Then,

$$N_0(k) = M(k) B^2(k+1) + N_1(k) B(k+1) - M(k) C^2(k+1) + F(k) C(k+1) + D(k), \tag{63}$$

$$N_1(k) = -2M(k) B(k+1) - 2M(k) C(k+1) + F(k). \tag{64}$$

The discriminant of the quadratic polynomial

$$-M(k)[p_{12}(k) - p_{12}(k+1)]^2 + N_1(k)[p_{12}(k) - p_{12}(k+1)] + N_0(k)$$

is

$$\Delta(k) = N_1^2(k) + 4M(k) N_0(k) = F^2(k) + 4M(k) D(k) = 4q_{11}(k) q_{22}(k) > 4\delta_{11}\delta_{22}. \tag{65}$$

Choose $\varepsilon = 4\overline{\delta}$ and $0 < \overline{\delta} < \delta_{11}\delta_{22}$, then $\Delta(k) > \varepsilon$.

$$\frac{N_1(k) - \sqrt{\Delta(k) - \varepsilon}}{2M(k)} < p_{12}(k) - p_{12}(k+1) < \frac{N_1(k) + \sqrt{\Delta(k) - \varepsilon}}{2M(k)}, \tag{66}$$

$$\frac{N_1(k)}{2} - \sqrt{q_{11}(k) q_{22}(k) - \overline{\delta}} < -\varepsilon_1 \Delta f_1(k) < \frac{N_1(k)}{2} + \sqrt{q_{11}(k) q_{22}(k) - \overline{\delta}}. \tag{67}$$

If inequality (66) is valid, then inequality (67) is satisfied. According to Lemma 3 (b), then

$$M_{Q_2} > \varepsilon/(4M) = \overline{\delta}. \tag{68}$$

According to expressions (59) and (68), M_{Q_1} and M_{Q_2} are larger than a positive constant.

Since every element of $Q(k)$ is bounded, then M_{Q_1} and M_{Q_2} are bounded. From Lemma 2, we can conclude that $Q(k)$ is uniformly bounded and positive definite.

Summing up the statement above, if the change rate of $f_1(k)$ satisfies inequality (44); the change rate of $f_1^2(k)$ and $f_2^2(k)$ satisfies inequalities (45), (46); in addition, there exists a uniformly bounded and positive definite matrix $P(k)$ which makes $Q(k)$ determined by eq. (51) uniformly bounded and positive definite, then according to Lemma 1, we can conclude that the closed loop system with origin as the equilibrium point is uniformly asymptotic stable.

Note 1. In Theorem 1, the condition $0 < \beta(k)/\hat{\beta}(k) \leqslant 2$ implies $\beta(k) \neq 0$. Since $\beta(k)$ belongs to the bounded closed convex set D, then $\beta(k) \in [\beta_{\min}, \beta_{\max}]$. Therefore, zero is not included in $[\beta_{\min}, \beta_{\max}]$. Because the projection algorithm (30), (31) guarantees $\hat{\beta}(k) \in [\beta_{\min}, \beta_{\max}]$, the estimation $\hat{\beta}(k)$ can be avoided to approximate zero.

6 Design of adaptive guidance law

According to eq. (12), if the vehicle flies along the reference trajectory, the tracking control input is given by

$$u_0(k) = \frac{-\ddot{a}_{D_0} + \dfrac{\dot{a}_{D_0}^2}{a_{D_0}} - 2\dfrac{a_{D_0}\dot{a}_{D_0}}{v_0} - \dfrac{2a_{D_0}^3}{v_0^2} + \dfrac{2a_{D_0}g^2}{v_0^2} - \dfrac{2a_{D_0}g}{r_0} - \dfrac{a_{D_0}v_0^2}{h_s r_0} + \dfrac{a_{D_0}g}{h_s} + \dfrac{a_{D_0}\ddot{C}_{D_0}}{C_{D_0}} - \dfrac{a_{D_0}\dot{C}_{D_0}^2}{C_{D_0}^2}}{\dfrac{2ga_{D_0}^2}{v_0^2} + \dfrac{a_{D_0}^2}{h_s}}. \tag{69}$$

Since the vehicle enters the atmosphere with hypersonic speed, the inertia is large. In order to reduce the tracking error of the piecewise linear drag acceleration vs. velocity profile, the logical integral is added in the neighborhood where the abrupt change of slope occurs. Considering that the velocity varies quickly during reentry, the logical integral is revised. To reduce the effect of previous errors on present states, errors of only the recent N steps are accumulated in the logical integral.

$$\begin{aligned}
&u_{li}^*(k) = -k_{li}\sum_{i=k-N}^{k} x(i),\\
&u_{li}(k) = \begin{cases} u_{li}^*(k) & v_1 - \Delta v_b \leqslant v \leqslant v_1 + \Delta v_a,\\ 0 & \text{otherwise,}\end{cases}\\
&k_{li} = \begin{cases} k_{li}^+ & x(k)\big[x(k) - x(k-1)\big] > 0,\\ k_{li}^- & x(k)\big[x(k) - x(k-1)\big] < 0,\end{cases}\\
&k_{li}^+ \geqslant k_{li}^- \geqslant 0, \quad \Delta v_a > 0, \quad \Delta v_b > 0,
\end{aligned} \tag{70}$$

where v_1 is the velocity at the first transition point of the reference drag acceleration profile. N, Δv_a, and Δv_b are chosen according to the vehicle's characteristic and the specific shape of the reference drag acceleration profile.

Combining expressions (29), (69) and (70), the adaptive guidance law of tracking the reference drag acceleration profile is

$$u(k) = u_0(k) + u_L(k) + u_{li}(k). \tag{71}$$

Since u is the vertical component of the lift-drag ratio, the bank angle follows from expression (4) as

$$\sigma = \cos^{-1}\left[\frac{(L/D)_V}{(L/D)}\right] = \cos^{-1}\left[\frac{u}{(L/D)}\right], \tag{72}$$

where (L/D) is the actual lift-drag ratio. Since the bank angle is limited by the upper and lower bounds, that is, $\sigma \in [\underline{\sigma}, \overline{\sigma}]$, then $u(k)$ should be limited by corresponding bounds, that is, $u(k) \in [\underline{u}(k), \overline{u}(k)]$.

7 Simulation example

The dynamics of a reentry vehicle are described by eqs. (1)—(3). The sampled period is $\Delta t = 0.1$ s. The parameters of the vehicle [16] are given by

$$m = 104305 \text{ kg}, \quad S = 391.22 \text{ m}^2,$$

$$C_L = -0.041065 + 0.016292\alpha + 0.00026024\alpha^2,$$

$$C_D = 0.080505 - 0.03026C_L + 0.86495C_L^2.$$

The purpose of guidance is to make the vehicle track the piecewise linear reference drag acceleration vs. velocity profile (Figure 1). The profile is within the corridor bounded by the maximum heat rate, the maximum overload, the maximum dynamic pressure and the equilibrium glide constraint. Noticeably, in Figure 1 the drag acceleration is the function of velocity, and the reentry is a process with velocity decreasing.

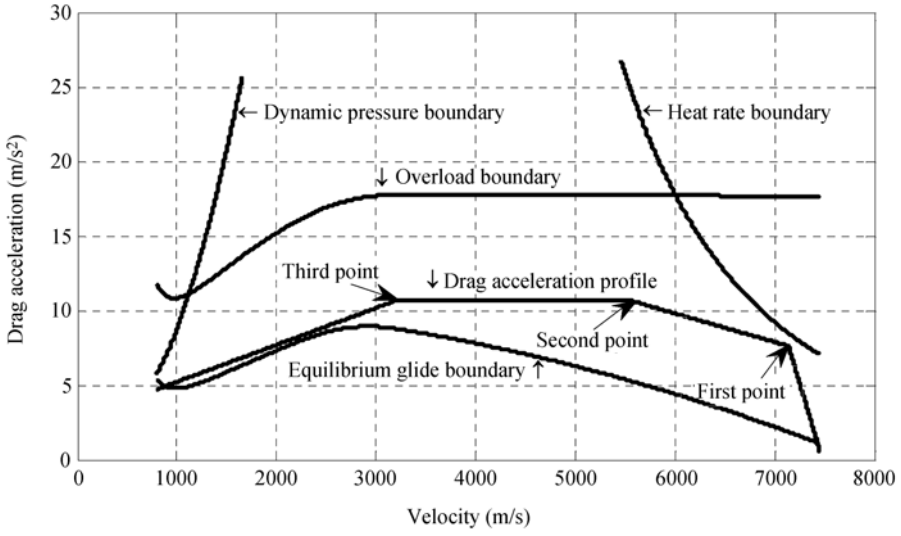

Figure 1 Reference drag acceleration vs. velocity profile within the reentry corridor.

7.1 Tracking control law + nonlinear differential golden-section control law

Choose the tracking control law and the nonlinear differential golden-section control law to make

up the control input as

$$u(k)=u_0(k)+u_L(k). \tag{73}$$

The corresponding bank angle can be obtained by expression (72). When this σ acts on the point-mass motion eqs. (1)—(3), the actual flight trajectory is obtained. Figure 2 gives the tracking of the reference drag acceleration vs. velocity profile when the input is given by eq. (73). The solid line represents the actual drag acceleration. The dashed line represents the reference drag acceleration. Figure 3 shows the tracking error history. Figures 2 and 3 show that the tracking is perfect except some overshoot at the first transition point. In Theorem 1, proper small constants δ_1, δ_2, δ_{11}, δ_{22}, $\overline{\delta}$, and ε_1 are chosen to satisfy requirements. During the simulation, the change rate of $f_1(k)$, $f_1^2(k)$, and $f_2^2(k)$ is recorded. The results show that inequalities (44)—(46) are satisfied during most of the reentry time.

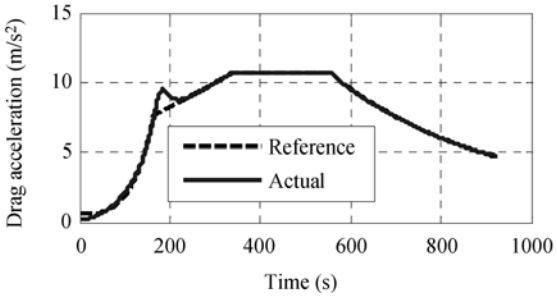

Figure 2 Tracking of the reference drag acceleration with the adaptive guidance law given by eq. (73).

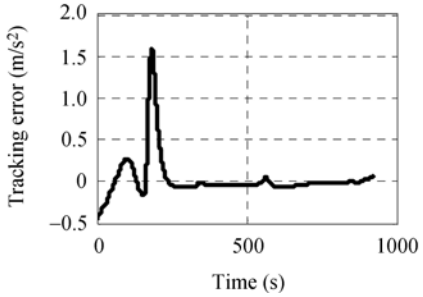

Figure 3 Tracking error with the adaptive guidance law given by eq. (73).

7.2 Tracking control law + nonlinear differential golden-section control law + logical integral control law

In order to reduce the tracking error near the first transition point, the logical integral control law is added. Considering that the velocity varies quickly during reentry, errors of only the recent N steps are accumulated. Using eqs. (71)—(72), the adaptive guidance law and the corresponding bank angle are obtained.

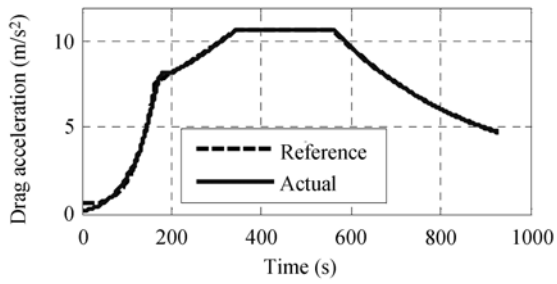

Figure 4 Tracking of the reference drag acceleration after the logical integral control law is added.

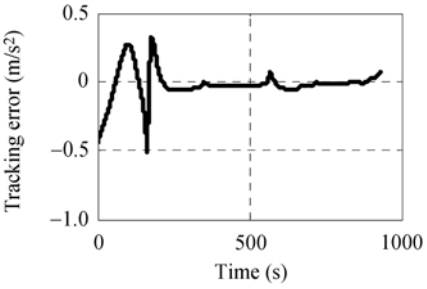

Figure 5 Tracking error after the logical integral control law is added.

Figure 4 shows the tracking of the reference drag acceleration vs. velocity. Figure 5 gives the corresponding error. It is obvious that after the logical integral is added, the tracking error near the first transition point decreases largely. The maximum tracking error is $|\Delta a_D| = 0.52$ m/s^2.

Figure 6 gives the bank angle history.

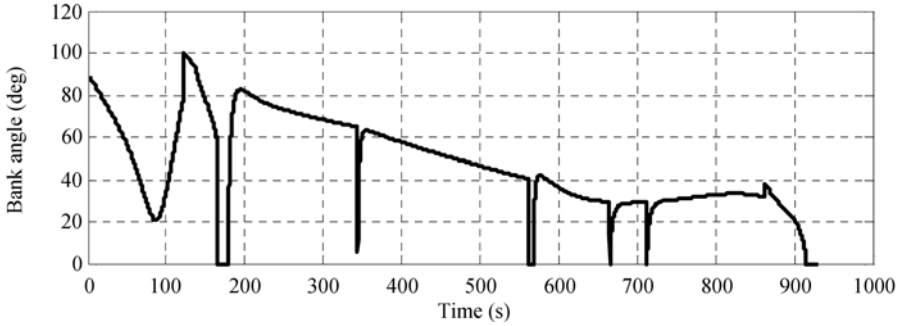

Figure 6 Bank angle history.

7.3 Comparing with the feedback linearization method

The adaptive guidance law is given by eq. (71). The feedback linearization method refers to refs. [3, 5—7, 16]. These two methods are compared by simulation in three cases. The first case is for nominal condition. The second is the case when the drag coefficient decreases 40 percent. The third is the case when time-varying navigation error exists. The height change rate caused by the inertial navigation system is $\delta\dot{h} = 5e^{0.005t}$ in the simulation. Figures 7—9 show that in three cases the adaptive guidance method is better than the feedback linearization one. For the feedback linearization method, the controller is designed by cancelling out the nonlinearity completely. When model error exists in the system, the control performance will fall down because the nonlinearity can't be cancelled exactly. For the adaptive guidance law based on the characteristic model, the controller is designed by estimating the parameters of the characteristic model on line. Therefore, the good tracking performance can be obtained even if large model error exists (see Figure 8). Since the drag acceleration derivative that includes the height change rate is used in the feedback linearization guidance law, the error of height change rate caused by navigation system has effect on the system. For the adaptive method presented in this paper, the derivative of the drag acceleration is not used so that the above disadvantage can be avoided. In Figure 9, the error of height change rate has little effect on the tracking error for the adaptive method but causes large tracking error for the feedback linearization method.

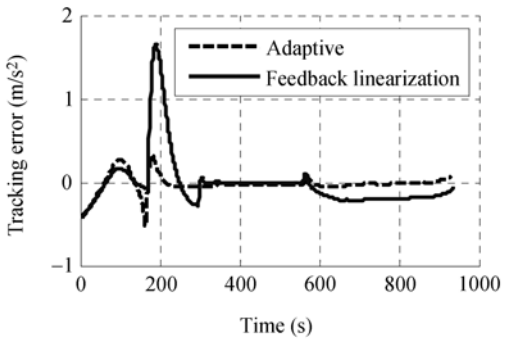

Figure 7 Tracking error in nominal case.

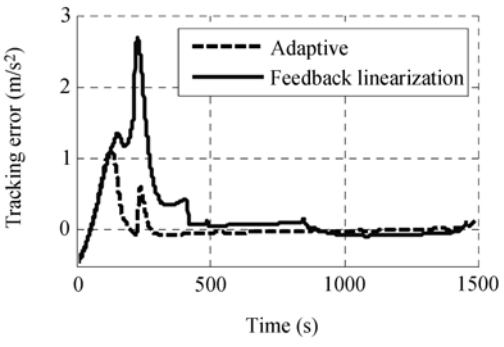

Figure 8 Tracking error when the drag coefficient decreases 40 percent.

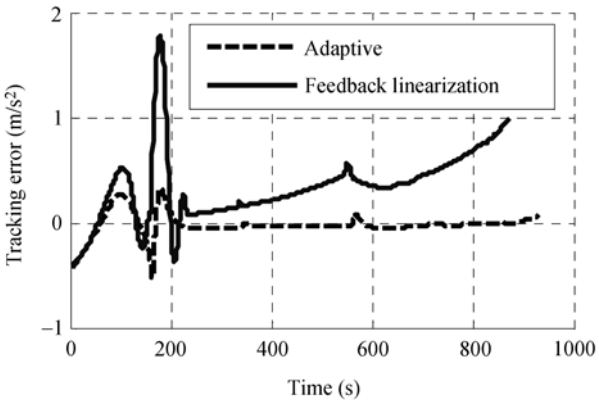

Figure 9 Tracking error when navigation error exists.

8 Conclusions

In this paper, the characteristic model is established and a new nonlinear differential golden-section adaptive control law is proposed. For the characteristic model described by the second order time-varying differential equation, when its parameters belong to a bounded closed convex set, the uniformly asymptotic stable sufficient condition of the closed loop system is obtained. The sufficiency is constraints on the change rate of parameters. The tracking control law, the nonlinear differential golden-section control law, and the revised logical integral control law are integrated to design an adaptive guidance law. For the nonlinear differential golden-section control presented in this paper, the large differential coefficient can be chosen so that the damping ratio is large which makes the tracking become stable quickly. The tracking error is reduced further after the logical integral is added. For the simulation example, during most of the time of reentry flight, inequalities (44)—(46) in Theorem 1 are satisfied. The simulation results show that the tracking performance of drag acceleration is obviously better for the adaptive guidance method than for the feedback linearization one. In addition, the control method proposed in this paper combining the nonlinear differential golden-section control law with the revised logical integral control law provides an idea for tracking problems with fast and abrupt change of slope.

Appendix The derivation of eq. (11)

Differentiating eq. (8)

$$\dot{g} = -2\dot{r}R_0^2 g_0 / r^3 = -2\dot{r}g / r. \tag{A1}$$

Differentiating eq. (1)

$$\ddot{h} = \dot{v}\sin\theta + v\dot{\theta}\cos\theta. \tag{A2}$$

Differentiating eq. (6)

$$\dot{\rho} = -(\dot{h}/h_s)\rho_0 e^{-h/h_s} = -(\dot{h}/h_s)\rho. \tag{A3}$$

Differentiating eq. (7)

$$\dot{a}_D = (\dot{C}_D / C_D + \dot{\rho}/\rho + 2\dot{v}/v)a_D. \tag{A4}$$

Using eq. (A3), the derivative of drag acceleration follows from eq. (A4) as

$$\dot{a}_D = (\dot{C}_D / C_D - \dot{h}/h_s + 2\dot{v}/v)a_D. \tag{A5}$$

Eq. (A5) is divided by a_D and then differentiated, eq. (A6) is derived.

$$\ddot{a}_D / a_D - \dot{a}_D^2 / a_D^2 = \ddot{C}_D / C_D - \dot{C}_D^2 / C_D^2 - \ddot{h} / h_s + 2\ddot{v} / v - 2\dot{v}^2 / v^2. \tag{A6}$$

Following from eq. (A6)

$$\ddot{a}_D = a_D(\dot{a}_D^2 / a_D^2 + \ddot{C}_D / C_D - \dot{C}_D^2 / C_D^2 - \ddot{h} / h_s + 2\ddot{v} / v - 2\dot{v}^2 / v^2). \tag{A7}$$

Combining eq. (A1), the derivative of $\dot{v}$ follows from eq. (9) as

$$\ddot{v} = -\dot{a}_D - g\dot{\theta}\cos\theta + 2g\sin\theta\dot{r} / r. \tag{A8}$$

Combining eqs. (1), (5), (9), (10), (A2), (A7) and (A8), eq. (11) is obtained.

1 She W X, Zhou F Q, Zhou J. Nonlinear variable structure guidance law. J Astr, 2003, 24(6): 638－641
2 Guo J G, Shui Z S, Zhou F Q, et al. Guidance law of reentry vehicle with terminal angular constraint. J Proj Rockets, Missiles and Guidance, 2006, 26(2): 1081－1083
3 Harpold J, Graves C, Graves C. Shuttle entry guidance. J Astr Sci, 1979, 27(3): 239－268
4 Leavitt J, Saraf A, Chen D T, et al. Performance of evolved acceleration guidance logic for entry (EAGLE). AIAA Technical Report, 2002－4456
5 Yang X L, Mease K D. Entry guidance and trajectory tracking error analysis. J Astr, 2004, 25(3): 283－288
6 Mease K D, Kremer J P. Shuttle entry guidance revisited. AIAA Technical Report, 92－4450
7 Lu P, Hanson J M. Entry guidance for the X-33 vehicle. J Spacecraft and Rockets, 1998, 35(3): 342－349
8 Wu H X. All-coefficient Adaptive Control Theory and Its Application. Beijing: National Defense Industry Press, 1990
9 Wu H X, Liu Y W, Liu Z H, et al. Characteristic modeling and the control of flexible structure. Sci China Ser F-Inf Sci, 2001, 44(4): 278－291
10 Hu J. All-coefficient adaptive reentry lifting control of manned spacecraft. J Astronautics, 1998, 19(1): 8－12
11 Wang X J. Spacecraft Entry and Return Technology. Beijing: Astronautics Press, 1991.
12 Sun D Q, Wu H X. Characteristic modeling and adaptive fuzzy control method of MIMO higher-order linear time-varying systems. J Astr, 2005, 26(6): 677－692
13 Wu H X, Wang Y, Xie Y C. Nonlinear golden-section adaptive control. J Astr, 2002, 23(6): 1－8
14 Sun D Q, Wu H X. Uniformly asymptotic stability of the 4th-order time-varying discrete systems. Contr Theory Appl, 2006, 23(6): 845－852
15 Xie Y C, Wu H X. The application of the golden section in adaptive robust controller design. Acta Automat Sin, 1992, 18(2): 177－185
16 Lu P. Entry guidance and trajectory control for reusable launch vehicles, AIAA Technical Report, 96－3700